Kidney International, Vol. 68 (2005), pp. 2694–2703

Calcium-binding proteins annexin A2 and S100A6 are sensors of tubular injury and recovery in acute renal failure

CHAO-WEN CHENG, ABDALLA RIFAI, SHUK-MAN KA, HAO-AI SHUI, YUH-FENG LIN, WEI-HWA LEE, and ANN CHEN

Graduate Institute of Life Sciences, Graduate Institute of Medical Sciences, Department of Internal Medicine, Department of Pathology, Tri-Service General Hospital, National Defense Medical Center, Taiwan, Republic of China; and Department of Pathology, Rhode Island Hospital, Rhode Island

Calcium-binding proteins annexin A2 and S100A6 are sensors of tubular injury and recovery in acute renal failure.

Background. Rise in cellular calcium is associated with acute tubular necrosis, the most common cause of acute renal failure (ARF). The mechanisms that calcium signaling induce in the quiescent tubular cells to proliferate and differentiate during acute tubular necrosis have not been elucidated.

Methods. Acute tubular necrosis induced in mice by single intravenous injection of uranyl nitrate and examined after 1, 3, 7, and 14 days. Renal function was monitored and kidneys were evaluated by histology, immunohistochemistry, Western blotting, in situ hybridization, and real-time reverse transcription-polymerase chain reaction (RT-PCR). Models of folic acid induced-ARF and ischemic/reperfusion (I/R) injury were similarly investigated.

Results. Analysis of mRNA expression of intracellular calcium and phospholipid-binding proteins demonstrated selective expression of *S100A6 and Annexin A2 (Anxa2)* in the renal cortex with marked elevation on day 3, and gradually decline on day 7 and further attenuation on day 14. Similarly, the expression of both proteins, as demonstrated by immunohistochemistry and Western blot analysis, was increased and reached the peak level on day 7 and then gradually declined by day 14. Vimentin, a marker of dedifferentiated cells, was highly expressed during the recovery phase. Combined in situ hybridization immunohistochemistry revealed colocalization of both S100A6 and Anxa2 with proliferating cell nuclear antigen (PCNA). The universality of this phenomenon was confirmed in two other mouse acute tubular necrosis models, the ischemic-reperfusion injury and folic acid-induced ARF.

Conclusion. Collectively, these findings demonstrate that S100A6 and Anxa2 expression, initiated in response to tubular injury, persist in parallel throughout the recovery process of tubular cells in acute renal failure.

Key words: acute tubular necrosis, S100A6, annexin A2, calcium-binding proteins.

Received for publication May 4, 2005
and in revised form June 22, 2005
Accepted for publication July 20, 2005

Acute tubular necrosis is the most common pathologic entity responsible for the clinical state of acute renal failure (ARF) [1, 2]. The two main causes of acute tubular necrosis are ischemic and toxic injuries [3]. In the latter type, a variety of renal environmental substances that include heavy metals such as mercury, lead, and uranium are known to cause ARF. Nephrotoxic acute tubular necrosis is histologically evident as epithelial cell necrosis, mainly in the proximal convoluted tubules, with preservation of the tubular basement membrane, and usually intact distal tubular segments [4].

Although severely damaged by toxin, the kidney has the ability to completely recover structurally and functionally. Normally, quiescent cells undergo dedifferentiation and regain their potential to divide after enhancement of DNA synthesis in acute tubular necrosis. Consequent to cell proliferation, the new cells differentiate to restore the functional integrity of the nephron [5]. Little is known of the mechanism(s) by which regeneration of renal tubules is mediated. The observations that hepatocyte growth factor (HGF), epidermal growth factor (EGF), and bone morphogenetic protein-7 (BMP-7) are among the potent regulators of kidney organogenesis and that these agents can also promote tubular regeneration after a variety of insults [6] are consistent with the idea that the regeneration process may be partially controlled by a mechanism similar to that operating during development.

Tubular cell calcium concentration and content are increased following acute renal injury induced by ischemic and toxic insults. The divalent calcium cation (Ca^{2+}) signaling system operate by binding to effector molecules, Ca^{2+} binding proteins, that mediate stimulation of numerous Ca^{2+} dependent processes such as transcription and cell proliferation. Two large families of the Ca^{2+} binding proteins are the annexins and the EF-hand motif S100 proteins [7]. The annexins are a family of phospholipid-binding proteins that share a common property of interacting with membranes and target molecules in a

Ca^{2+}-dependent manner [8, 9]. S100 proteins represent the largest subgroup in the EF-hand Ca^{2+} binding protein family. A unique feature of S100 proteins is that individual members are localized in specific cellular compartments from which some are able to relocate upon Ca^{2+} activation, thus transducing the Ca^{2+} signal in a temporal and spatial manner by interacting with different targets specific for each S100 protein [10]. Interactions between annexins and S100 proteins are now known to include several members of these protein families.

During the course of our studies on global gene expression profiling in a mouse model of uranyl nitrate–induced ARF, we observed dramatic up-regulation in the expression of S100A6 (calcyclin) and annexin A2. Accordingly, we postulated these interactive effector molecules might play a role in the pathophysiology of ARF and their expression might be useful biomarkers of the temporal events and processes of the tubular epithelial cell in acute tubular necrosis.

METHODS

Animal models

Uranyl nitrate–induced acute tubular necrosis. Female 8-week-old C57BL/6 mice were purchased from the National Laboratory Animal Breeding and Research Center (Taipei, Taiwan). All mice received a single tail vein injection of uranyl nitrate [$(UO_2\ (NO_3)_2 \cdot 6\ H_2O$] (100 μg in 100 μL of 5% $NaHCO_3$). The mice were sacrificed at 0, 3, 7, and 14 days after the injection. Blood and urine were collected for clinical evaluation, and kidneys were removed for molecular and histopathology studies. Samples intended for histopathology were fixed in formalin according to a standard protocol.

Ischemic/reperfusion (I/R) injury. This model was induced as previously described [11]. Briefly, bilateral I/R injury was generated in female Balb/c mice (25 to 30 g) by occluding the renal pedicles with microvascular clamps for 30 minutes under ketamine-xylazine anesthesia. Completeness of ischemia was verified by blanching of the kidneys, signifying the stoppage of blood flow. The blood flow to the kidneys was reestablished by removal of the clamps (reperfusion) with visual verification of blood return. Mice subjected to sham operation (identical treatment except that the renal pedicles were not clamped) were used as controls. During the procedure, animals were well hydrated and their body temperature maintained with an adjustable heating pad. At 4, 12, 24, and 72 hours postischemia, mice were killed, and their kidneys were removed for RNA extraction.

Folic acid–induced ARF. Folic acid (240 mg/kg) was administered into female Balb/c mice (25 to 30 g) in vehicle (0.2 mL of 0.3 mol/L $NaHCO_3$) or vehicle only by intraperitoneal injection [12]. The control kidneys were analyzed before folic acid or vehicle administration. The mice were sacrificed, and their kidneys were collected at 1, 3, 7, and 14 days at each time point.

Renal function

Blood samples collected through the retro-orbital venous plexus were centrifuged ($3000 \times g$, 10 minutes), and the supernatant containing the serum was withdrawn and stored at $-70^{\circ}C$ until assayed. Renal function was assessed by measuring the elevation in plasma levels of creatinine and blood urea nitrogen (BUN). These analyses, which utilized Fuji DRI-CHEM 3030 (Fuji Photo Film Co. Ltd., Tokyo, Japan), were obtained within 15 minutes once the serum samples thawed.

Renal histopathology

The formalin-fixed renal tissues were dehydrated in a graded series of ethanol solutions and embedded in paraffin as described elsewhere [13]. Three micron sections were obtained and stained with hematoxylin and eosin. For typical lesions of acute tubular necrosis, tubular cell necrosis, of which some of them were sloughed into the tubular lumina accompanied by casts [14]. Quantitative analysis of renal tubular necrosis was performed by optical microscopy. Briefly, 100 intersections were examined for each kidney and a score from 0 to 3 was given for each tubular profile involving an intersection: 0, normal histology; 1, tubular cell swelling, brush border loss, nuclear condensation, with up to one third of tubular profile showing nuclear loss; 2, as for score 1, but greater than one third and less than two thirds of tubular profile shows nuclear loss; and 3, greater than two thirds of tubular profile shows nuclear loss. The total score for each kidney was calculated by addition of all 100 scores with a maximum score of 300. There was also evidence of tubular cell regeneration, it was defined as flattened epithelial cells with hyperchromatic nuclei and mitotic figures [14]. Quantitative analysis of renal tubular regeneration was performed by optical microscopy. Briefly, 100 intersections were examined for each kidney and a score from 0 to 3 was given for each tubular profile involving an intersection: 0, normal histology; 1, flattened epithelial cells with hyperchromatic nuclei and mitotic figures with up to one third of tubular profile showing hyperchromatic nuclei and mitotic figures; 2, as for score 1, but greater than one third and less than two thirds of tubular profile shows hyperchromatic nuclei and mitotic figures; and 3, greater than two thirds of tubular profile shows hyperchromatic nuclei and mitotic figures. The total score for each kidney was calculated by addition of all 100 scores with a maximum score of 300.

Table 1. Polymerase chain reaction (PCR) primers

	5′ primers	3′ primers
S100A6	CGCTTCTTCTAGCCCAGTCAT	ACTGGATTTCACCGAGAGAGG
S100A10	AGACCACTTCACAAAGGAGGAC	GCCTATTTCTTCCCCTTCTGCT
S100A11	GACTGAGAGATGCATTGAGTCC	ACAGTTCAGGTCCAGCTTCTTC
Annexin A2	GTGGATGAGGTCACCATTGTC	GTCGGTTCCTTTCCTCTTCAC
Annexin A1	GGGACTTGGAACAGATGAAGAC	GTCTCTCCCCTTTCTCCTTTCT
Annexin A11	GTCCCTCCTTATGGAATCTATCC	AGTATCCTGGGTAACTTGGCACT
β-actin	GACGGCCAGGTCATCACTAT	ACATCTGCTGGAAGGTGGAC

Reverse-transcriptase polymerase chain reaction (RT-PCR)

Total RNA was extracted with Trizol reagent (Invitrogen Corporation, Carlsbad, CA, USA) from total kidney. For first-strand cDNA synthesis, 1.5 μg of total RNA was used in a single-round RT reaction. The reaction mixture consisted of 0.9 μL Oligo $(dT)_{12–18}$ primer, 1.0 mmol/L deoxynucleoside triphosphate (dNTP), 1× first-strand buffer, 0.4 mmol/L dithiothreitol (DTT), 80 U RNase-out recombinant ribonuclease inhibitor, and 300 U superscript II RNase H (Invitrogen Corporation). PCR was run by using 1 μL of the RT reaction mixture as the template, 0.4 μmol/L of gene-specific primers, 1× PC2 buffer, 0.25 mmol/L dNTP, and 1.5 U KlenTaq DNA polymerase (Ab Peptides Inc., St. Louis, MO, USA). The amplification was carried out at 94°C for 2 minutes, then for 25 cycles at 94°C for 30 seconds, 58°C for 45 seconds, and 72°C for 30 seconds, followed by a final extension at 72°C for 10 minutes. The primers are listed in Table.1. β-actin and each target gene product were electrophoretically separated on a 1% agarose gel and stained with ethidium bromide. Real-time PCR was performed on an ABI Prism 7700 Sequence Detection System (Applied Biosystems, Foster City, CA, USA). All of the probes and primers were Assays-on-Demand Gene expression products (Applied Biosystems). Real-time PCR reactions were using 10 μL of cDNA, 12.5 μL of TaqMan Universal PCR Master Mix (Applied Biosystems), 1.25 μL of the specific probe/primer mixed in a total volume of 25 μL. The thermal cycler conditions were as follows: 1 × 2 minutes 50°C, 1 × 10 minutes 95°C, 40 cycles denaturation (15 seconds 95°C) and combined annealing/extension (1 minute 60°C). Amplifications were normalized to β-actin using $2^{-\Delta\Delta CT}$ method (Applied Biosystems).

Western blot analysis

Each sample was run on a 12% sodium dodecyl sulfate-polyacrylamide gel electrophoresis (SDS-PAGE) gel. The gel was electro-blotted onto a nitrocellulose membrane, incubated for 1 hour in 20 mL of blocking buffer [Tris-buffered saline (TBS), 5% skim milk], washed three times in TBS with 0.1% Tween-20 (TBST), and incubated with goat anti-S100a6, goat anti-Anxa2, rabbit anti-proliferating cell nuclear antigen (PCNA) antibodies (Santa Cruz Biotechnology Inc., Santa Cruz, CA, USA) at 4°C overnight. Blots were washed three times and incubated horseradish peroxidase–conjugated rabbit antigoat or goat antirabbit antibodies (Pierce, Rockford, IL, USA) for 1 hour at room temperature. Membranes were washed three times, and the membrane-bound antibody detected was incubated chemiluminescent reagent plus (Perkin Elmer Life Sciences, Boston, MA, USA) and captured on x-ray film.

Immunohistochemical staining

Immunohistochemical staining was performed on formaldehyde-fixed and paraffin-embedded tissues using the avidin-biotin immunoperoxidase method [15]. The antibodies used included goat anti-annexin A2, goat anti-S100A6, rabbit anti-PCNA (Santa Cruz Biotechnology Inc., Santa Cruz, CA) and goat anti-vimentin (ICN Biomedicals Inc., Irvine, CA, USA). Paraffin was removed from sections and followed by rehydration. Endogenous peroxidase activity was quenched and the sections were blocked with 1% wt/vol bovine serum albumin (BSA) in phosphate-buffered saline (PBS) for 1 hour. The sections were then incubated with a 1:100 dilution of goat polyclonal anti-S100A6 antibody in PBS. After incubation with a biotinylated secondary antibody (Dako, Glostrup, Denmark), the tissue sections were treated with an avidin-biotin-peroxidase complex (Dako). The reaction was visualized by use of a 3,3′-diaminobenzidine (DAB) chromogen (Dako) following tissue counterstaining with hematoxylin. For double staining, the slides were incubated with the first antibody, which was demonstrated by the ABC method described above and microwaved with citrate buffer. Subsequently, the slides were incubated with the second antibody for 1 hour, which was visualized by an alkaline phosphatase–mediated reaction as described previously [16]. Quantitative analysis for S100A6, annexin A2, and PCNA was performed at high power (200×) by optical microscopy. Twenty randomly selected cortical fields were examined in each section. Preliminary examinations established that the renal tubules were the major portion that was positively stained. A proportion score and intensity score were assigned. The proportion score represented the estimated the percentages of positive tubular cells (1, 0%

to 20%; 2, 20% to 40%; 3, 40% to 60%; 4, 60% to 80%; and 5, 80% to 100%). The intensity score represented the estimated average staining intensity of tubular cells (0, none; 1, weak; 2, intermediate; and 3, strong). The overall amount of positive staining was then expressed as the sum of the proportion and intensity scores.

Immunoelectron microscopic study

Samples were fixed in a mixture of 4% paraformaldehyde and 0.5% glutaraldehyde in PBS, pH 7.4, and prepared routinely for electron microscopy with final embedding in LR White resin as described previously [15]. Ultrathin sections were cut and placed on nickel grids. Primary (goat anti-annexin A2) (1:100) (Santa Cruz Biotechnology) and secondary antibodies (1:40) (gold-labeled) (British Biocell International, Cardiff, UK) were applied. The presence and localization of the 10 nm gold particles were examined under an electron microscope.

In situ hybridization

In brief, 3 μm paraffin sections were mounted on charged glass slides and stored in airtight boxes at 70°C. Riboprobes were generated by using a pGEMT-EASY plasmid containing cDNA insert of mouse annexin A2 and S100A6 to generate antisense transcripts for in situ hybridization. In vitro transcription was carried out using a commercial kit. For in situ hybridization, Dig-labeled mRNAs were diluted 100-fold in hybridization buffer containing 2 mmol/L ethylenediaminetetraacetic acid (EDTA) (pH 7.5), 20 mmol/L Tris (pH 7.5), 0.6 mol/L NaC1, 2× Denhardt's solution, 20% dextran sulfate, 0.1 mg/mL tRNA, and 0.2 mol/L DTT. After deparaffinization, kidney sections were digested with 20 μg/mL proteinase K in PBS for 20 minutes. Sections were acetylated using 0.25% acetic anhydride in 0.1 mol/L triethanolamine for 10 minutes. A volume of 25 to 50 μL of hybridization mixture was placed on each section and covered with a siliconized glass coverslips. Hybridization was performed in moist chambers at 42°C for 16 hours. Coverslips were removed by washing in 1× saline sodium citrate (SSC) at room temperature and 0.2× SSC for 10 minutes at room temperature. Slides were then washed in 0.05 × SSC for 10 minutes at room temperature followed by a washing step in 0.025× SSC for 30 minutes at 37°C. After rinsing the slides in maleic buffer (0.1 mol/L maleic acid, pH 7.5, and 0.15 mol/L NaCl) for 1 minute at room temperature and blocking with 1× blocking buffer 60 minutes then incubated with riboprobes (1:200) at 42°C overnight. Wash with maleic buffer and develop with nitro blue tetrzolium chloride/5-bomo-4-chloro-3-indolyl-phosphate (NBT/BCIP) solution in dark. With double staining, slides were microwaved with citrate buffer and treated for immunohistochemistry as reported previously in this article.

Statistical analysis

All results were expressed as means ± standard deviation. Comparisons between two groups were made by unpaired Student *t* test. Differences among multiple groups were determined with the one-way analysis of variance (ANOVA) using Tukey's method for post hoc analysis. $P < 0.05$ was considered statistically different.

RESULTS

Clinical and pathologic features

In mice that received a single dose of uranyl nitrate, the levels of serum creatinine rapidly increased to reach 1.554 ± 0.371 mg/dL by day 3, as compared to normal controls (0.13 ± 0.03 mg/dL) (Fig. 1A). This difference was significant ($P < 0.05$). Thereafter, creatinine levels gradually declined. By day 14 following uranyl nitrate injection, the creatinine levels (0.29 ± 0.19 mg/dL) approached control values (Fig. 1A).

A similar trend and significance (Fig. 1B) was observed for serum BUN 127.85 ± 11.76 mg/dL on day 3 and 26.53 ± 8.76 mg/dL on day 14, compared to 24.58 ± 1.78 mg/dL in normal controls ($P < 0.05$).

Microscopic examination of renal tissue sections from the mice that received uranyl nitrate showed focal necrosis of renal tubules 3 days after injection (Fig. 1D and G), followed by a more diffuse and intense pattern on day 7 (Fig. 1E and G). Regeneration of renal tubules was noted on day 7 (Fig. 1H). On day 14 the histologic alterations were mild and had been mostly replaced by regenerating tubules (Fig. 1F and H) and a normal background (Fig. 1A).

Immunohistochemical staining of renal section with antivimentin, a cellular dedifferention marker, showed the proximal tubular cells undergo cell dedifferentiation to reenter the cell cycle during the 14 days of disease progression. In normal kidney cells, vimentin expression was restricted to podocytes of glomeruli and fibroblasts in the interstitium (Fig. 2A). However, the regenerating tubular cells of the acute tubular necrosis mouse model strongly expressed the vimentin protein on day 7 (Fig. 2C). A gradual decline in the protein level occurred thereafter and then declined gradually on day 14 (Fig. 2D).

Expression of S100 and annexin in the kidney

The expression of genes encoding S100A6, S100A10, S100A11, annexin A2, annexin A1, and annexin A11 was examined by using regular RT-PCR followed by quantification by real-time RT-PCR. As shown in Figure 3, there was an increase of S100A6 and annexin A2 in the progressive of uranyl nitrate–induced acute tubular necrosis. In contrast, there was no significant change in the expression of S100A10, S100A11, annexin A1, and annexin A11. These results indicate that during the period

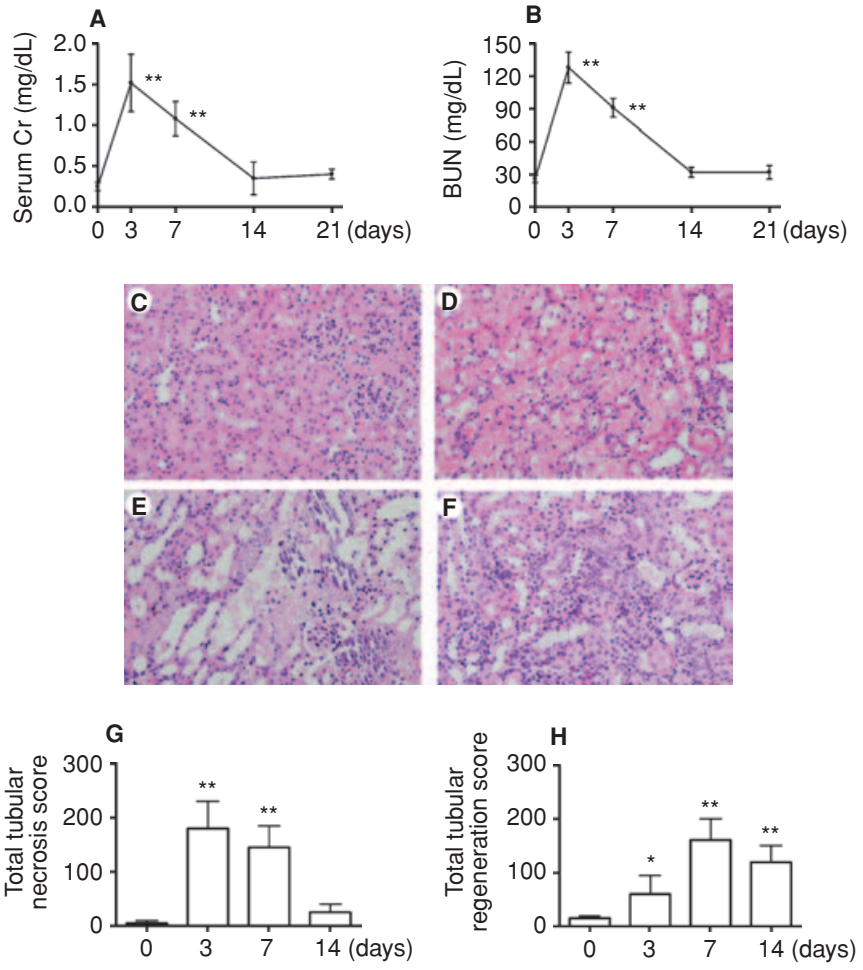

Fig. 1. Clinical and pathologic features. Levels of serum creatinine (Cr) (*A*) and blood urea nitrogen (BUN) (*B*) after the uranyl nitrate induction of nephrotoxic acute tubular necrosis (day 0). Both creatinine and BUN increased significantly to a maximum on day 3 ($P < 0.01$), then gradually approached the baseline value by day 14. Data are mean ± SD. $^{**}P < 0.01$ vs. control. Representative sections from renal tissue prior to uranyl nitrate induction on day 0 (normal) (*C*), and following induction, on days 3 (*D*), 7 (*E*), and 14 (*F*) (hematoxylin and eosin, original magnification, 200×). The quantitative analysis represents the degree of renal tubular necrosis (*G*) and regeneration (*H*) during the progressive of uranyl nitrate–induced acute tubular necrosis.

of dedifferentiation and regeneration in uranyl nitrate–induced acute tubular necrosis, the Ca^{2+}-binding proteins S100A6 and annexin A2 are selectively associated with the induction and recovery process.

Expression of S100A6 and annexin A2 proteins in the kidney

To examine the cellular distribution and association of S100A6 and annexin A2 with ARF, we performed immunohistochemical staining. Paraffin-embedded renal sections from control and from uranyl nitrate–induced mice kidneys were harvested at timed intervals (0, 3, 7, and 14 days) after induction. The expression of S100A6 and annexin A2 results indicated that in the kidneys of control animals (day 0), the S100A6 (Fig. 4A) and annexin A2 (Fig. 4E) are expressed in a very limited number of renal tubular epithelial cells (<0.1%). However, the expression of S100A6 and annexin A2 increased significantly at 7 day after induction. At this time point, both the number of the renal tubular epithelial cells expressing S100A6 (Fig. 4C) and annexin A2 (Fig. 4G) and the intensity of their staining increased significantly. Expression of S100A6 (Fig. 4B) and annexin A2 (Fig. 4F) at day 3

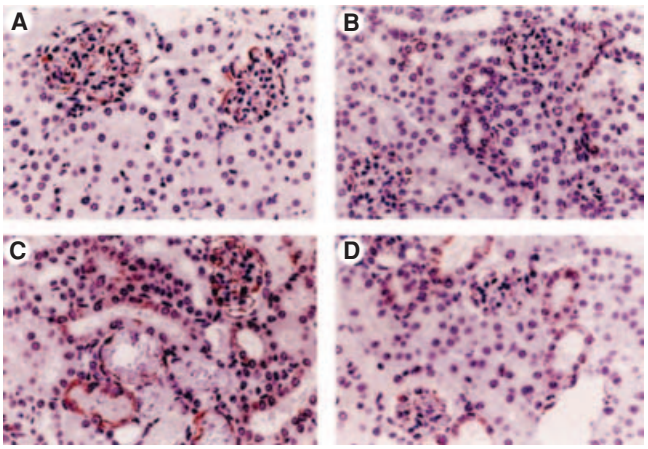

Fig. 2. Dedifferentiation of proximal tubular cells in uranyl nitrate–induced acute tubular necrosis. Paraffin-embedded mouse kidney sections were examined for expression of vimentin, a marker of cellular dedifferentiation, by immunohistochemical staining. (*A*) Normal tissue prior to uranyl nitrate induction. (*B*) Expression at 3 days postinduction showing enhanced tubular staining. (*C*) Expression 7 days postinduction showing maximum staining and distribution in proximal tubular cells. (*D*) Decline in expression at day 14 (original magnification, 400×).

was greater than that of the control but considerably less than that at day 7. S100A6 and annexin A2 staining in kidney sections after day 7 indicates considerable variation, with some tubules demonstrating no labeling in any cell, whereas in some tubules all cells expressed S100A6 and annexin A2. The results indicate that S100A6 and annexin A2–positive cells are primarily located in the inner cortical and outer medullary regions (corticomedullary junction) of the kidney, a region that contains the S_3 segment of the proximal tubules. Similarly, the expression of annexin A2 protein in the kidney showed the same pattern as that of the S100A6, with the intensity of protein staining being less than the S100A6 by Western blot analysis (Fig. 4I). Besides, the expression pattern of these proteins in the kidney sections was similar to that of vimentin during the recovery phase. For confirmation of the intracellular localization of annexin A2, immune electron microscopy was performed on renal samples taken at day 7 and showed an intracytoplasmic distribution of the protein in the regenerating tubular epithelial cells (Fig. 5).

Co-localization of S100A6, annexin A2, and PCNA in acute tubular necrosis kidney

Acute tubular necrosis involves both the loss of epithelial cell polarity and the onset of proliferative response. Therefore to determine the relevance of the S100A6 and annexin A2 to these processes, we examined the proliferative status of renal tubular epithelial cells and coexpression of these two proteins. Kidney sections, obtained on day 7 after uranyl nitrate treatment, were double stained with ribo-probes against either S100A6 or annexin A2 mRNA and with the antibody against PCNA, a marker of cell proliferation. The majority of cells (>80%) expressing S100A6 (Fig. 6A, dark blue color) and annexin A2 (Fig. 6B, dark blue color) and were also PCNA-positive (Fig. 6, red color). Semiquantitative scoring analysis revealed concordant patterns of abundance among the three proteins (Fig. 6C). Besides, colocalization of both S100A6 and annexin A2 was evaluated by double staining. Most of the regenerating tubular cells were found to express the proteins simultaneously (Fig. 6D).

S100A6 and annexin A2 expression in I/R injury and folic acid–induced ARF mouse models

To determine the general relevance of S100A6 and annexin A2 expression to the pathophysiology of acute renal failure, we examined their expression in two different mouse models. In the nephrotoxin model of folic acid induced ARF, the temporal pattern of S100A6 and annexin A2 expression (Fig. 7A and C) was reminiscent of uranyl nitrate model that peaked between day 3 and 7 and returned to normal level by day 14. The expression of PCNA also peaked between day 3 and day 7 (Fig. 7E). More important, in the rapid ARF model of I/R injury,

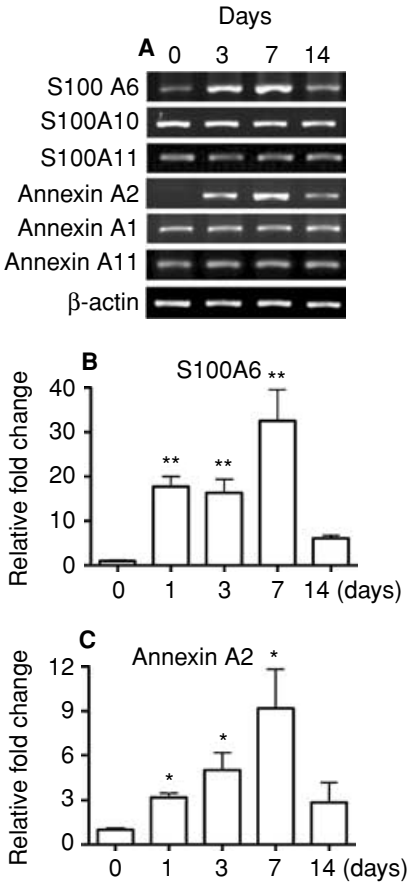

Fig. 3. Selective increase in the expression of S100A6 and annexin A2 in uranyl nitrate–induced acute tubular necrosis. For comparing the differential expression among the different members in the families of S100 and annexins: S100A6, S100A10, S100A11, and annexin A2, annexin A1, and annexin A11 were examined by semiquantitative reverse transcription-polymerase chain reaction (RT-PCR) during the progression of uranyl nitrate–induced acute tubular necrosis. Aliquots of 5 μL were sampled from each PCR product after 25 cycles (*A*). Time course quantitative expression level of S100A6 and annexin A2 were measured by real-time RT-PCR (*B*). The quantitative analysis represents fold change of S100A6 and annexin A2 relative to control and the results presented as units normalized to β-actin mRNA. Data represent mean ± SD. $^{*}P < 0.05$ vs. control; $^{**}P < 0.01$ vs. control.

the expression of S100A6 and annexin A2 (Fig. 7B and D) were elevated early (12 hours) and declined to normal level (72 hours) as a respective sensor of tubular injury and recovery.

DISCUSSION

In the present studies, by quantitative real-time RT-PCR, in situ hybridization, immunoblot analysis, and immunohistochemistry, we demonstrated that annexin A2 and S100A6 Ca^{2+} binding proteins were modulated in a temporal pattern concomitant with the initiation and recovery of ARF. In the nephrotoxin uranyl nitrate model elevated levels of both annexin A2 and S100A6 were significantly elevated at 3 days postinduction and returned

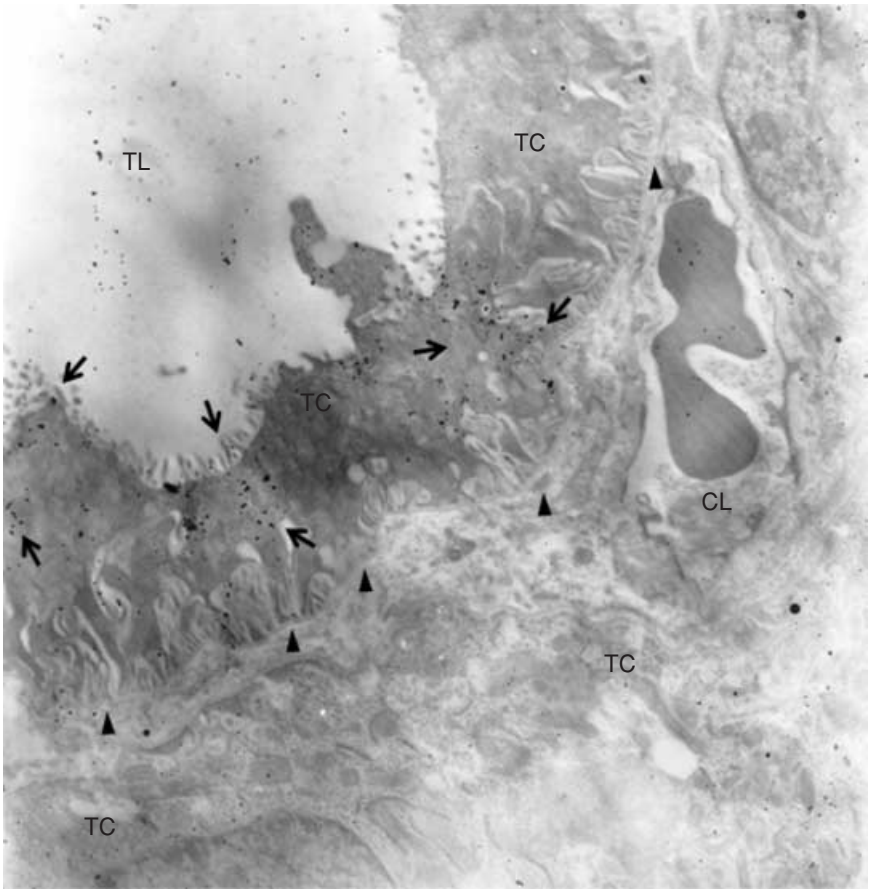

Fig. 5. Ultrastructural immunolocalization of annexin A2 proteins in the regenerating tubule. Immune electron microscopy of annexin A2 in the kidney tissue of uranyl nitrate acute tubular necrosis model. Arrows indicate regenerating tubular epithelial cells containing annexin A2 which was demonstrated by gold particles (original magnification, 6000×). Arrowheads indicate tubular basement membrane. Abbreviations are: CL, capillary; TC, tubular cell; TL, tubular lumen.

to normal level by 14 days. By comparison, the I/R renal injury prompted similar but much earlier expression that peaked between 12 and 24 hours and attenuated to normal levels by 72 hours. Thus these findings suggest these proteins could be involved in the proliferative process that results in repopulation of tubular cells and recovery from ARF.

Annexins are a family of 13 proteins known to bind phospholipids in a Ca^{2+}-dependent way. They are widely expressed proteins and share a similar structure characterized by a conserved C-terminal domain with Ca^{2+} binding sites and a variable N-terminal domain. Depending on Ca^{2+} concentration, they have been reported to participate in a variety of membrane-related events such as exocytosis, endocytosis, apoptosis, cell proliferation, and binding to cytoskeletal proteins [8, 9, 17]. On the other hand, the S100 protein family is also a multigenic family of low molecular mass (9 to 11 kD) calcium binding proteins [18]. Within cells, S100 proteins have been implicated in the regulation of protein phosphorylation, some enzyme activities, the dynamics of cytoskeleton components, transcription factors, Ca^{2+} homeostasis, and cell proliferation and differentiation. Certain S100 members are released into the extracellular space by an unknown mechanism. Extracellular S100 proteins are known to enhance cellular survival, differentiation, proliferation, apoptosis, and stimulate or inhibit inflammatory cells [19]. Thus, there is the potential of a large complex variety of Ca^{2+} signaling that results from the cooperative actions of these two specific Ca^{2+} binding protein families.

Changes in the genomic expression of S100A6 and annexin A2 have not been previously described for the nephrotoxin type of acute tubular necrosis. The observation that both genes were overexpressed almost in parallel throughout the clinical course is consistent with the suggestion that the Ca^{2+} binding proteins may be closely related. Depletion of cellular adenosine triphosphate (ATP) leads to an increase in the cytosolic Ca^{2+} concentration in cells [20, 21]. ATP depletion also inhibits Ca^{2+} ATPase and Na-K-ATPase. The inhibition of these enzymes leads directly or indirectly to increased cytoplasmic Ca^{2+} [22, 23]. This elevated high cytoplasmic concentration may increase the expression of Ca^{2+} binding proteins. Consistent with this suggestion is the observation of a tenfold increase in detectable S100A6 transcription 1 day after renal I/R injury [18]. S100A6 was initially identified by differential screening as mRNA species that was induced in G_0 when quiescent hamster kidney cells were stimulated to proliferate by addition of serum. Thus, it has been suggested that S100A6 could play

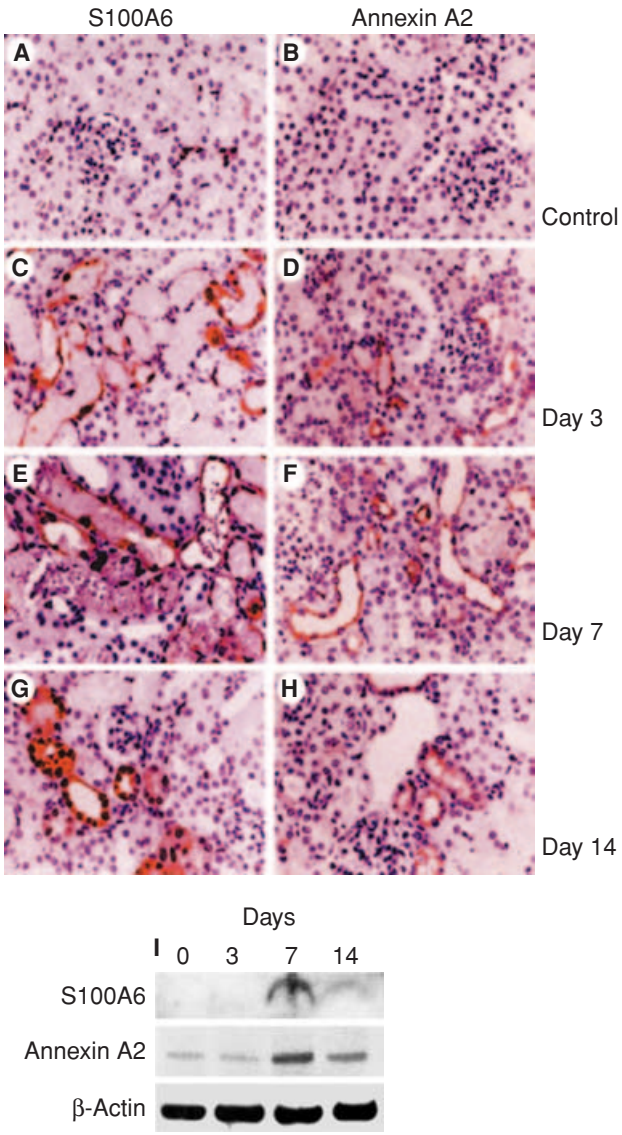

Fig. 4. Localization and distribution of S100A6 and annexin A2 proteins in uranyl nitrate–induced acute tubular necrosis. Immunohistochemical staining of renal tissue from controls showing low levels of S100A6 (*A*) and annexin A2 (*B*) proteins. Following uranyl nitrate induction, up-regulation of S100A6 and annexin A2 proteins observed in cortical tubules on days 3 (*C* and *D*), further enhancement of the S100A6 and annexin A2 proteins as punctuate distribution in regenerative renal tubules on day 7 (*E* and *F*) and these proteins persisted to day 14 (*G* and *H*) (original magnification, 400×). Western blot analysis of renal cortical regions protein extracts (*I*).

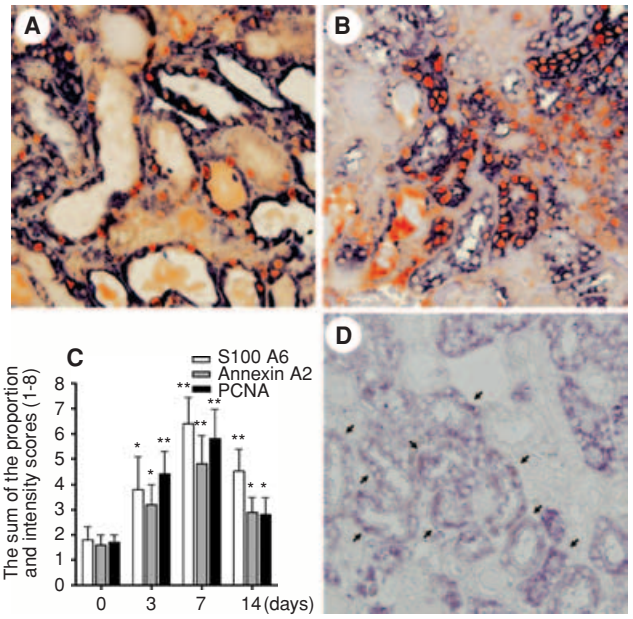

Fig. 6. S100A6 and annexin A2 overexpression in proliferating proximal tubular cells in uranyl nitrate–induced acute tubular necrosis. For detection the relationship of S100A6, annexin A2, and proliferating cell nuclear antigen (PCNA), double staining for combined in situ hybridization and immunohistochemical analysis was used. Paraffin-embedded mouse kidney sections at day 7 in uranyl nitrate–induced mice were examined for expression of S100A6 (*A*) and annexin A2 (*B*) by in situ hybridization (black blue) and PCNA (red) by immunohistochemical staining (original magnification, 400×). Semiquantitative analysis for S100A6, annexin A2, and PCNA during the course of acute tubular necrosis (*C*). Data are mean ± SD. $^{*}P < 0.05$ vs. control; $^{**}P < 0.01$ vs. control. By immunohistochemical double staining, the S100A6 (red) and annexin A2 (black blue) were expressed simultaneously in most of the regenerating tubular cells (*D*). Arrows indicate regenerating tubular epithelial cells containing S100A6 and annexin A2 (original magnification, each 400×).

a role in the regulation of renal cell proliferation and shift into the G_1 phase of the cell cycle [18]. Our findings of coexpression of S100A6 and PCNA (Fig. 6) in the uranyl nitrate model are also concordant with these suggestions.

Several intracellular proteins have been identified as potential targets of S100A6 signaling pathways on the basis of Ca^{2+}-dependent binding to the protein in vitro. These include annexins A2 and A6, glyceraldehyde 3-phophate dehydrogenase (GAPDH), caldesmon, tropomysin, Siah-interacting protein (SIP) and SGT1 [24, 25]. Annexin A2 is the major cellular substrate for the tyrosine kinase encoded by *src* oncogene, and can interact with S100A6 in vitro [26–28]. In vivo it can form a high affinity heterotetrameric complex with p11, another member of the S100 protein family [27]. Interestingly, annexin A2 genomic expression is up-regulated during the mammalian cell cycle, with maximal expression occurring as cells enter S phase, a subsequent decline in expression during S phase, and the rapid synthesis of annexin A2 mRNA as G_2 commences [29].

Analogous to their role in dividing cell lineages, augmented expression of annexin A2 and S100A6 in postischemic injury, may reflect a conserved response of the surviving proximal tubule epithelial cells in an attempt to reserve the transcriptional machinery for activation of genes required to reenter the cell cycle. Examination of renal tissue at different times during the progression of acute tubular necrosis confirmed that the production of both the S100A6 and annexin A2 proteins increased immediately after induction and reached a plateau in

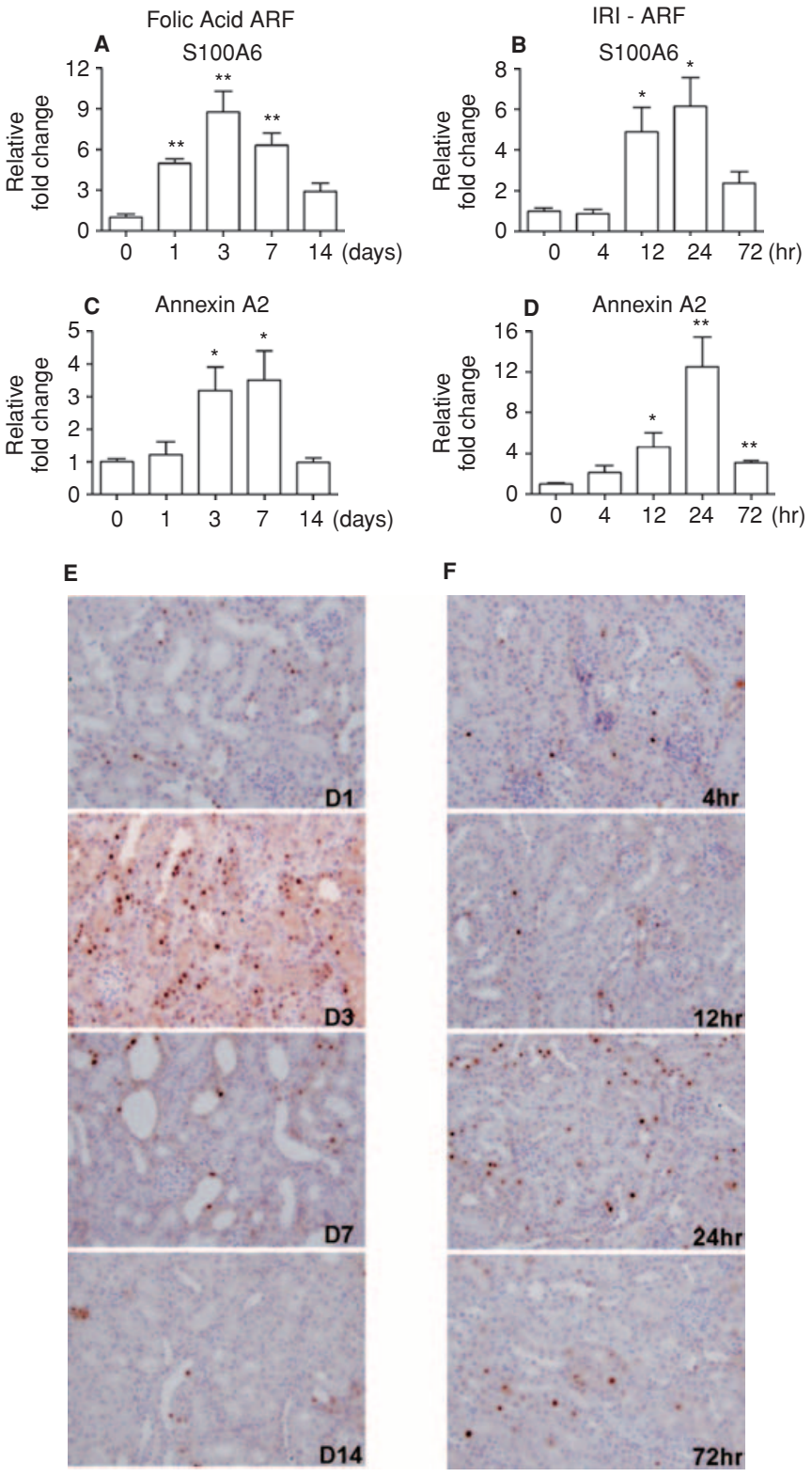

Fig. 7. Comparative analysis of S100A6 and annexin A2 gene expression with proliferating cell nuclear antigen (PCNA) staining in folic acid–induced acute renal failure (ARF) and ischemic/reperfusion (I/R) injury (IRI). Real-time reverse transcription-polymerase chain reaction (RT-PCR) analysis for the level of S100A6 (*A*) and annexin A2 (*B*) in folic acid–induced ARF mice model and the changes of S100A6 (*C*) and annexin A2 (*D*) in I/R injury model. Data are mean ± SD. $^{*}P < 0.05$ vs. control; $^{**}P < 0.01$ vs. control. Expression of PCNA during the course of acute tubular necrosis in each model. In parallel with the expression of S100A6 and annexin A2, the PCNA-positive cells was dominantly expressed in day 3 of folic acid–induced ARF mice model (*E*), and the 24 hours in I/R injury model (*F*) (original magnification, 200×).

the damaged regenerating segments of proximal tubules. S100A6 and annexin A2 could thus play a role in the regulation of renal cell proliferation and regeneration in the recovery process in nephrotoxic and I/R acute tubular necrosis. Whether these events occur in the human condition remains to be established, although the similarities between the mouse model used in the present study and human acute tubular necrosis make such a suggestion

realistic. Further studies are needed to correct to patients with human acute tubular necrosis.

ACKNOWLEDGMENTS

The abstract of this work has been presented in the Third World Congress of Nephrology June 26–30, 2005 in Singapore. We thank Mr. Yao-Wen Hung (Institute of Preventive Medicine, National Defense Medical Center, Taipei, Taiwan) for his technical assistance in immune electronic microscopy. This study was supported by grants from the National Health Research Institutes (NHRI-EX92-9137SN), the National Science Council (NSC-93-2320-B016-026), and the Ministry of Economic Affairs (94-EC-17-A-20-S1-028), Taiwan, Repubic of China.

Reprint requests to Dr. Ann Chen, Department of Pathology, Tri-Service General Hospital, National Defense Medical Center No. 325, Sec. 2, Cheng-Gung Road, Taipei, Taiwan, ROC.
E-mail: doc31717@ndmctsgh.edu.tw

REFERENCES

1. Lieberthal W, Koh JS, Levine JS: Necrosis and apoptosis in acute renal failure. *Semin Nephrol* 18:505–518, 1998
2. Lim IK, Lee KH, Han BD, *et al*: Uranyl nitrate induced polyuric acute tubular necrosis in rats. *Yonsei Med J* 28:38–48, 1987
3. Lieberthal W, Nigam SK: Acute renal failure. II. Experimental models of acute renal failure: Imperfect but indispensable. *Am J Physiol Renal Physiol* 278:F1–F12, 2000
4. Bulger RE: Renal damage caused by heavy metals. *Toxicol Pathol* 14:58–65, 1986
5. Toback FG: Regeneration after acute tubular necrosis. *Kidney Int* 41:226–246, 1992
6. Nigam S, Lieberthal W: Acute renal failure. III. The role of growth factors in the process of renal regeneration and repair. *Am J Physiol Renal Physiol* 279:F3–F11, 2000
7. Heizmann CW: Calcium-binding proteins: Basic concepts and clinical implications. *Gen Physiol Biophys* 11:411–425, 1992
8. Raynal P, Pollard HB: Annexins: The problem of assessing the biological role for a gene family of multifunctional calcium and phospholipid-binding proteins. *Biochim Biophys Acta* 1197:63–93, 1994
9. Morgan RO, Fernandez MP: Annexin gene structures and molecular evolutionary genetics. *Cell Mol Life Sci* 53:508–515, 1997
10. Donato R: Intracellular and extracellular roles of S100 proteins. *Microsc Res Tech* 60:540–551, 2003
11. Mishra J, Ma Q, Prada A, *et al*: Identification of neutrophil gelatinase-associated lipocalin as a novel early urinary biomarker for ischemic renal injury. *J Am Soc Nephrol* 14:2534–2543, 2003
12. Long DA, Woolf AS, Suda T, *et al*: Increased renal angiopoietin-1 expression in folic acid-induced nephrotoxicity in mice. *J Am Soc Nephrol* 12:2721–2731, 2001
13. Chen A, Sheu LF, Ho YS, *et al*: Experimental focal segmental glomerulosclerosis in mice. *Nephron* 78:440–452, 1998
14. Kumar V, Abbas AK, Fausto N: *Robbins & Cotran Pathologic Basis of Disease*, 7th ed., 2005, pp 994–995
15. Chen A, Chou WY, Ding SL, *et al*: Glomerular localization of nephritogenic protein complexes on a nonimmunologic basis. *Lab Invest* 67:175–185, 1992
16. Ricono JM, Xu YC, Arar M, *et al*: Morphological insights into the origin of glomerular endothelial and mesangial cells and their precursors. *J Histochem Cytochem* 51:141–150, 2003
17. Camors E, Monceau V, Charlemagne D: Annexins and Ca2+ handling in the heart. *Cardiovasc Res* 65:793–802, 2005
18. Lewington AJ, Padanilam BJ, Hammerman MR: Induction of calcyclin after ischemic injury to rat kidney. *Am J Physiol* 273:F380–F385, 1997
19. Donato R: S100: A multigenic family of calcium-modulated proteins of the EF-hand type with intracellular and extracellular functional roles. *Int J Biochem Cell Biol* 33:637–668, 2001
20. Snowdowne KW, Borle AB: Effects of low extracellular sodium on cytosolic ionized calcium. Na+-Ca2+ exchange as a major calcium influx pathway in kidney cells. *J Biol Chem* 260:14998–14507, 1985
21. Kribben A, Wieder ED, Wetzels JF, *et al*: Evidence for role of cytosolic free calcium in hypoxia-induced proximal tubule injury. *J Clin Invest* 93:1922–1929, 1994
22. Weinberg JM: The cell biology of ischemic renal injury. *Kidney Int* 39:476–500, 1991
23. Bonventre JV: Mechanisms of ischemic acute renal failure. *Kidney Int* 43:1160–1178, 1993
24. Nowotny M, Spiechowicz M, Jastrzebska B, *et al*: Calcium-regulated interaction of Sgt1 with S100A6 (calcyclin) and other S100 proteins. *J Biol Chem* 278:26923–26928, 2003
25. Filipek A, Jastrzebska B, Nowotny M, *et al*: CacyBP/SIP, a calcyclin and Siah-1-interacting protein, binds EF-hand proteins of the S100 family. *J Biol Chem* 277:28848–28852, 2002
26. Klee CB: Ca2+-dependent phospholipid- (and membrane-) binding proteins. *Biochemistry* 27:6645–6653, 1988
27. Filipek A, Gerke V, Weber K, *et al*: Characterization of the cell-cycle-regulated protein calcyclin from Ehrlich ascites tumor cells. Identification of two binding proteins obtained by Ca2(+)-dependent affinity chromatography. *Eur J Biochem* 195:795–800, 1991
28. Osborn M, Johnsson N, Wehland J, *et al*: The submembranous location of p11 and its interaction with the p36 substrate of pp60 src kinase in situ. *Exp Cell Res* 175:81–96, 1988
29. Chiang Y, Schneiderman MH, Vishwanatha JK: Annexin II expression is regulated during mammalian cell cycle. *Cancer Res* 53:6017–6021, 1993